CIRP Annals - Manufacturing Technology 67 (2018) 523–526

Contents lists available at ScienceDirect

CIRP Annals - Manufacturing Technology

journal homepage: http://ees.elsevier.com/cirp/default.asp

Enhanced dimensional measurement by fast determination and compensation of geometrical misalignments of X-ray computed tomography instruments

Wim Dewulf (2)[a,*], Massimiliano Ferrucci [a,b], Evelina Ametova [a], Petr Heřmánek [c], Gabriel Probst [a], Bart Boeckmans [a], Tom Craeghs [b], Simone Carmignato (2)[c]

[a] KU Leuven, Mechanical Engineering Department, Celestijnenlaan 300, 3001 Leuven, Belgium
[b] Materialise NV, Technologielaan 15, 3001 Leuven, Belgium
[c] University of Padua, Department of Management and Engineering, Stradella San Nicola 3, Vicenza, Italy

ARTICLE INFO

Article history:
Available online 4 May 2018

Keywords:
Metrology
X-ray
Compensation

ABSTRACT

Full geometrical alignment of CT instruments remains a complicated endeavor. This paper therefore presents a fast and comprehensive method for determination and compensation of geometrical misalignments. First, a reference object, consisting of spheres mounted on a carbon fiber tube, is X-ray imaged at different angular positions. Subsequently, the misalignment parameters of the CT instrument are determined by minimizing the residual errors between observed and modelled sphere center coordinates. Finally, the FDK-based tomographic reconstruction algorithm is adapted to account for the determined misalignment parameters. The paper discusses the fundamentals of the approach and provides an experimental validation of its performance.

1. Introduction

X-ray computed tomography (CT) is increasingly accepted for dimensional quality control of industrial parts [1]. Nevertheless, various error sources [2] contribute to uncertainty in the CT measurement results and undermine the application of CT for critical industrial measurement tasks. Misalignments in the CT instrument geometry can introduce significant errors in CT measurements [3]. While methods for the measurement and compensation of CT geometrical misalignments are available in the literature [4], their implementation typically relies on physical adjustment of the CT instrument components—a complicated and time-consuming endeavor that can lead to increased errors if not performed correctly. In this study, we present a fast and comprehensive method for measurement and software compensation of geometrical misalignments in a cone-beam CT instrument. The method is first applied to simulated CT measurements on an industrial component. Then, the method is validated on experimental CT measurements on an industrial CT instrument.

2. Cone-beam CT instrument geometry

The geometry of a cone-beam CT instrument can be defined by seven geometrical parameters describing the relative position and orientation of the three main components: X-ray source, sample stage axis of rotation, and flat-panel detector. Parameterization of the instrument geometry is illustrated in Fig. 1. The X-ray source focal spot **S** is the origin of a global coordinate frame. The global Y axis is parallel to the sample stage axis of rotation and is positive upwards. The global Z axis is given by the line from the origin that intersects the axis of rotation orthogonally and is positive away from the axis of rotation. The global X axis follows the right hand rule. Position of the sample stage axis of rotation is given by $\mathbf{R} = (0, 0, z_R)$. Detector position is given by the coordinate location of its geometrical center $\mathbf{D} = (x_D, y_D, z_D)$. The orientation of the detector is defined by three extrinsic Euler rotation angles θ, φ, η about axes parallel to the global X, Y, and Z axes, respectively, albeit with the center of rotation located at **D** and in the following order: (1) η, (2) φ, (3) θ. Hence, the instrument geometry can be fully described by 7 geometrical parameters: x_D, y_D, z_D, z_R, η, φ, and θ. Conventional tomographic reconstruction of data acquired by cone-beam CT

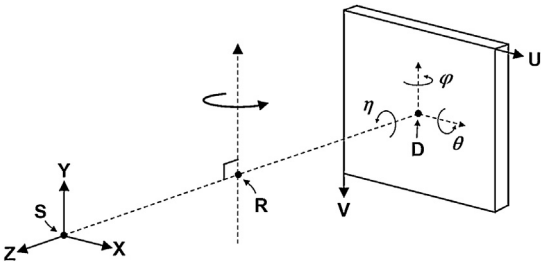

Fig. 1. Parameterization of the CT instrument geometry.

* Corresponding author.
E-mail address: wim.dewulf@kuleuven.be (W. Dewulf).

https://doi.org/10.1016/j.cirp.2018.04.124
0007-8506/

with circular scanning trajectory assumes a nominal alignment of the instrument. In a nominally aligned CT instrument, the magnification axis coincides with the global Z axis and intersects the detector at its geometrical center; z_D therefore, the full instrument geometry can be described by z_R and z_D.

3. Method

The proposed method for measurement and compensation of geometrical misalignments consists of three major steps, summarized in Fig. 2. Radiographs of a reference object consisting of spheres are acquired at different angular positions (1). The seven CT geometrical parameters are determined by tracking the positions of the sphere center coordinates (2). Radiographs of workpiece(s) are acquired at the same position of the rotation stage and are subsequently reconstructed using a new flexible-geometry tomographic reconstruction algorithm for compensation of instrument misalignments (3). Since kinematic errors can result in non-repeatable positioning and tilts of the sample stage, the sample stage should not be translated between steps (1) and (3).

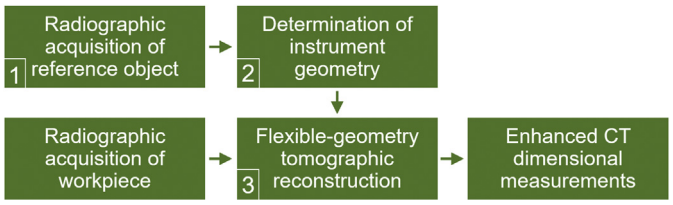

Fig. 2. Proposed method for enhanced CT dimensional measurements by measurement and compensation of instrument misalignments.

3.1. Reference object

The Computed Tomography Calibration Tube (CT^2), developed at the University of Padua, is used as the reference object [5]. The CT^2 consists of 49 grade 10 (ISO 3290-1) hardened stainless steel spheres (M = 48 reference spheres and 1 marking sphere) affixed along the outer circumference of a carbon fiber tube (Fig. 3). Spheres are arranged along ten 'rings' at various heights along the tube cylindrical axis. Sphere numbers within each ring increase counter-clockwise. Numbering continues along subsequent rings in the negative Y direction. The center position of each reference sphere in a local coordinate frame, the origin of which is at the geometrical center of the sphere arrangement, is measured by tactile coordinate measuring machine (CMM), MPE = 2 + L/300 μm, where L is the measured length in mm. In this study, the CT^2 was imaged at N = 720 equally spaced rotation positions of the stage.

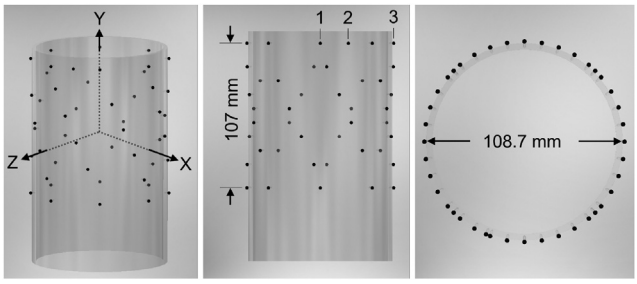

Fig. 3. The Computed Tomography Calibration Tube (CT^2) reference object for measurement of CT instrument geometry.

3.2. Geometrical measurement procedure

The CT instrument geometry is determined by least-squares minimization of reprojection errors. For each radiograph of the reference object $n = 1, 2, \ldots, N$ at its respective rotation position α_n of the stage, the observed center projection coordinates $(u_{obs,m}, v_{obs,m})$ of spheres $m = 1, 2, \ldots, M$ are determined by way of a dedicated image analysis procedure [6]. A separate ray-tracing algorithm provides a corresponding set of modelled sphere center projection coordinates (u_{mod}, v_{mod}) given an initial set of the seven instrument geometrical parameters and six "nuisance" parameters describing the position and orientation of the reference object in the instrument. Reprojection error given by the sum of squared residuals between modelled and observed center projection coordinates. Constrained minimization in conjunction with global optimization tool *Global Search* [7] are employed to minimize the reprojection error by iteratively adapting, i.e. 'solving', the seven instrument and six reference object geometrical parameters in the ray-tracing model.

3.3. FlexCT

The most common methods for CT reconstruction of data acquired by cone-beam CT with circular scanning trajectory are based on the Feldkamp–Davis–Kress algorithm (FDK) [8]. FDK is an extension of the filtered back-projection algorithm (FBP), originally developed for parallel-beam geometries, to the geometry of cone-beam CT instruments. In FBP-type reconstruction methods, radiographs are filtered independently and then back-projected onto the voxel space to calculate a three-dimensional X-ray attenuation map of the measurement volume. Processing of radiographs and back-projection are geometry-dependent procedures and their conventional implementation requires nominal alignment of the CT instrument components.

The flexible-geometry tomographic reconstruction algorithm (FlexCT) developed at KU Leuven is a modification of conventional FDK to non-nominal instrument geometries. The measured instrument parameters from the geometrical measurement procedure in Section 3.1 are used to redefine the preprocessing of radiographs, i.e. pre-weighting and the back-projection geometry. The output of FlexCT is a volumetric grey value model of X-ray attenuation, which can be easily imported into volumetric analysis software.

4. Validation

The efficacy of the proposed method is tested on simulated CT measurements of a pipe connector and subsequently validated experimentally on CT measurements of a ball plate (Fig. 4).

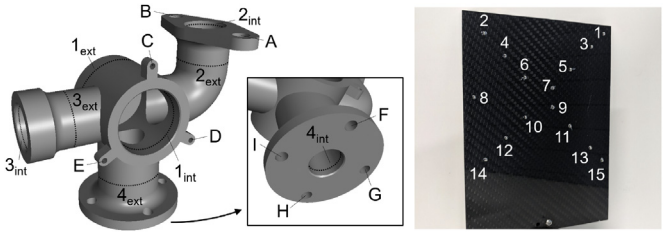

Fig. 4. CAD model of the pipe connector measured by simulated CT (left) and ball plate for experimental validation (right).

4.1. Simulations

Features of interest on the pipe connector are internal and external diameters of Sections 1–4; and distance between flange holes within the same flange. Three reference spheres (not illustrated) are added at the extremities of the measurement volume for voxel rescaling. An in-house forward projection model is used for generation of the radiographic images. Acquisition of the workpiece is first simulated under nominal alignment of the CT components (where $z_R = -364.282$ mm and $z_D = -1027.003$ mm), henceforth referred to as the 'aligned acquisition'. Radiographic images of the workpiece are then generated under five 'misaligned acquisition' geometries (Table 1). Projections were acquired at 3600 equally spaced angular positions of the rotation stage. For each misaligned geometry, a

Table 1
Instrument geometrical parameters for five misaligned acquisitions of the test object.

		Simulated parameters						
		Z_R/mm	x_D/mm	y_D/mm	Z_D/mm	θ/°	φ/°	η/°
Simulation	1	−364.282	−0.259	−1.370	−1027.003	−0.6756	−0.0989	−0.7867
	2	−362.874	0.623	1.882	−1029.583	0.5886	−0.8324	0.9238
	3	−364.815	−1.492	0.829	−1026.446	−0.3776	−0.5420	−0.9907
	4	−365.325	1.754	−0.059	−1023.660	0.0571	0.8267	0.5498
	5	−366.396	−0.529	1.201	−1025.213	−0.6687	−0.6952	0.6346

Table 2
Solved instrument geometrical parameters from implementation of the geometrical measurement procedure on five simulated misaligned acquisitions of the reference object.

		Solved parameters						
		Z_R/mm	x_D/mm	y_D/mm	Z_D/mm	θ/°	φ/°	η/°
Simulation	1	−364.262	−0.259	−1.370	−1026.948	−0.6753	−0.0989	−0.7867
	2	−362.854	0.623	1.882	−1029.527	0.5884	−0.8317	0.9238
	3	−364.799	−1.492	0.829	−1026.400	−0.3775	−0.5414	−0.9907
	4	−365.305	1.754	−0.059	−1023.605	0.0572	0.8261	0.5498
	5	−366.374	−0.529	1.202	−1025.152	−0.6685	−0.6946	0.6346

separate 720-projection acquisition of the CT^2 is also simulated. The geometrical measurement procedure in Section 3.2 is performed on the radiographs from each misaligned acquisition of the CT^2 to provide the set of solved geometrical parameters in Table 2.

Tomographic reconstruction assuming the nominal CT geometry is applied to the aligned and misaligned acquisitions of the pipe connector using Inspect-X reconstruction software (Nikon, UK). Dual center of rotation estimation in Inspect-X is applied for nominal reconstructions. Discrepancies in source-to-rotation axis distance (z_R) and source-to-detector distance (z_D) between nominal and misaligned acquisition geometry can be partially corrected by implementing voxel rescaling [9]. Voxel scaling factors for each misaligned acquisition of the pipe connector are determined from center-to-center distance measurements on the three reference spheres. A linear regression curve is fit to CT measurements of sphere center-to-center distances plotted as a function of their respective simulated values. Voxel scaling factors applied to reconstructed volumes from each misaligned acquisition are as follows, in order of simulation number: (1) 0.998, (2) 0.992, (3) 1.003, (4) 1.006, (5) 1.009. Reconstruction on the five misaligned acquisitions is also performed using FlexCT, the geometrical parameters of which are adapted to the measured values from Table 2.

The features of interest on the pipe connector are measured on the nominally reconstructed datasets without and with voxel scaling, henceforth 'nominal' and 'rescaled', and on the FlexCT-reconstructed datasets. Results are compared to equivalent measurements from nominal reconstruction of the aligned acquisition. Volumetric grey value models are imported into VGStudio MAX 3.0 (Volume Graphics, GmbH). An iso-surface is generated by applying advanced 'local' thresholding. Four inner diameters and four external diameters are measured by least-squares fitting cylinders to the respective surfaces. The position of each flange hole is defined as the intersection of a cylinder fit to the hole surface and a plane fit to the mating face of the respective flange. Ten hole-to-hole distances are measured: AB, CD, DE, CE, FG, FH, FI GH, GI, and HI. Errors of the measured values from the equivalent measurements on the aligned dataset are shown in Fig. 5 for diameter errors (left) and for distance errors (middle).

While voxel rescaling provides reductions in both diameter and distance measurement errors, it does not account for all geometrical misalignments as indicated by the further reductions of all errors to below 1 μm in FlexCT reconstructed datasets. Also, in the surface comparison (Fig. 5 right), extremities of the pipe connector still exhibit errors after voxel rescaling, yet not with FlexCT.

4.2. Experimental validation

The method is applied to CT measurements on a 450 kV CT instrument (Nikon XT H 450). The workpiece (Fig. 4 right) consists of 15 grade 20 chrome steel 2.5 mm diameter spheres arranged on a carbon fiber plate in a dedicated pattern. Sphere positions on the workpiece were measured by CMM with a MPE of 2 + L/400 μm, where L is the measured length in mm. A set of 720 radiographs of the CT^2 was acquired for measuring the geometry of the test instrument at a position of the sample stage chosen to maximize the detector coverage of the projected workpiece. The solved geometrical parameters for this position of the sample stage are shown in Table 3. The CT instrument was measured without applying any intentional misalignments.

Table 3
Measured geometrical parameters of 450 kV CT instrument at a given position of the sample stage.

Parameter						
Z_R/mm	x_D/mm	y_D/mm	Z_D/mm	θ/°	φ/°	η/°
−355.631	0.078	1.314	−1026.694	0.298	0.230	0.076

A set of 3142 radiographs of the workpiece was acquired at the same sample stage position as the radiographic acquisition of the CT^2. Reconstruction of the workpiece is performed on Inspect-X under nominal reconstruction geometry (where z_R = 355.978 mm and z_D = 1028.451 mm are the values given by the CT instrument) and on FlexCT under the measured geometry shown in Table 3. The nominally reconstructed data is evaluated without and with voxel scaling for comparison. A voxel scaling factor of approximately 1.0005 is obtained by applying the same procedure described in Section 3 on the nominally reconstructed 720-radiograph acquisition of the CT^2. Dual center of rotation estimation in Inspect-X is applied prior to nominal reconstruction.

Sphere center-to-center distances, sphere radii, and sphere form are measured on volumetric grey value models of the workpiece obtained from nominal, rescaled, and FlexCT reconstructions. The volumetric grey value models are converted into surface models, which are then converted to point clouds of three-dimensional surface coordinates by applying a surface sampling at

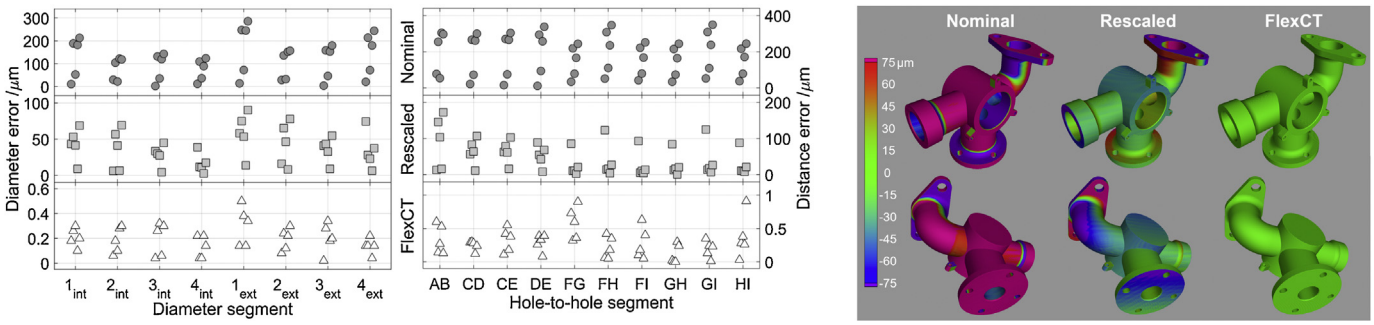

Fig. 5. Diameter measurement errors (left) and flange hole distance errors (middle) and comparison of surface models (right) for nominal, rescaled, and FlexCT reconstructed misaligned-acquisition datasets of the pipe connector.

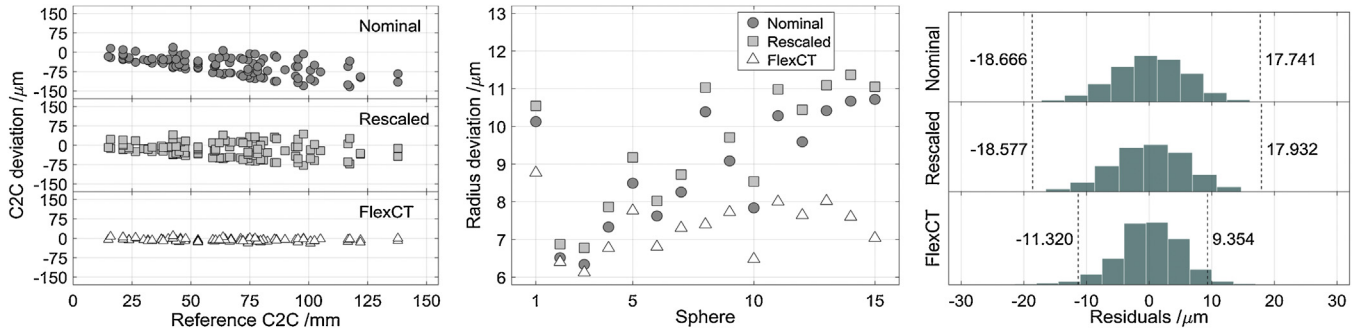

Fig. 6. Measurement errors for nominal, rescaled, and FlexCT reconstructed datasets: deviations in measured sphere center-to-center (C2C) distances (left), errors in measured sphere radii (middle), and sphere fit residual histograms for all spheres as an indicator for reconstructed sphere form (right). Vertical dashed lines denote the 2.5% and 97.5% quantiles corresponding to the lower and upper boundaries for 95% of sphere fit residuals.

intervals of 1 voxel along each coordinate direction. The cloud of point coordinates is further analyzed in MATLAB (Mathworks, Inc.). For each sphere in the reconstructed workpiece, a sphere is least-squares fit to the point coordinates belonging to the surface of that sphere. The distance between the centers is measured for all combinations of sphere pairs in nominal, rescaled, and FlexCT reconstructed datasets and compared to the equivalent CMM-measured (reference) distances.

Center-to-center distance (C2C) errors relative to the reference distances are shown in Fig. 6 (left). Errors in C2C measurements for the nominal dataset were as high as approximately 136 μm and exhibited a length dependence, indicating a scaling error in the voxel size. Rescaling the voxel size removed the length-dependence and reduced the maximum error to approximately 78 μm. The C2C measurements in the FlexCT reconstructed dataset exhibit a further improvement from the rescaled dataset, reducing maximum error to approximately 21 μm. These results indicate that, assuming correct skew compensation by Inspect-X center of rotation procedure, voxel rescaling does not account for the effects that out-of-plane detector angular misalignments θ and φ have on CT measurements [3].

Errors in measured radii are shown in Fig. 6 (middle) for each sphere in the reconstructed datasets. Radius errors were below 12 μm for all reconstructed datasets. Voxel size rescaling increased radius errors by as much as approximately 0.7 μm from equivalent radii in the nominal dataset. Radius errors in the FlexCT reconstructed dataset were consistently smaller by as much as 3.7 μm. Deviations in radius errors among all spheres were smaller in the FlexCT reconstructed dataset than in both nominal and rescaled datasets. Radius errors varied by 4.4 μm in the nominal dataset, by 4.6 μm in the rescaled dataset, and by 2.6 μm in the FlexCT dataset.

Sphere fit residuals between sphere surface coordinates and fit sphere are used as a measure of reconstructed sphere form. Histograms of sphere fit residuals from all spheres in each reconstructed dataset are shown in Fig. 6 (right). Dashed vertical lines denote the 2.5% and 97.5% quantiles, corresponding to the lower and upper boundaries, respectively, for 95% of all sphere fit residuals. Voxel rescaling did not significantly change sphere form errors, while sphere fit residuals in FlexCT reconstructed spheres were significantly lower.

5. Conclusions

A fast method is proposed for measurement and compensation of geometrical misalignments of the CT instrument. Measurement of the instrument geometrical parameters is achieved by least-squares minimization of reprojection errors from the acquisition of a dedicated reference object. Measured misalignments are compensated by modifying a flexible-geometry tomographic reconstruction algorithm for enhanced CT measurements.

The proposed procedure is applied to simulated acquisitions of an industrial component, namely a pipe connector. The method is further validated experimentally on the separate acquisition of a workpiece. The acquired datasets are reconstructed by conventional means, i.e. assuming aligned instrument geometry with and without voxel rescaling, and compared to the equivalent results after applying the proposed compensation methodology. Center-to-center distance measurement errors in the experimental acquisition of a workpiece were reduced from a maximum of approximately 136 μm under nominal reconstruction without voxel rescaling and a maximum of approximately 78 μm with voxel rescaling to below 22 μm under the proposed method. Sphere radius errors were consistently reduced after compensation. Variations in sphere error after compensation varied by 2.6 μm, while the same errors under conventional reconstruction varied by 4.4 μm and 4.6 μm without and with voxel rescaling, respectively. Residuals between reconstructed sphere surfaces and fit spheres were also significantly reduced under the compensation methodology.

In this study, the proposed method is shown to significantly reduce the effects of instrument misalignments on CT dimensional measurements. Another important observation in this study is the ineffectiveness of voxel rescaling to resolve these same effects. Voxel rescaling is often termed 'scale calibration'—a convention that could potentially mislead some to assume the procedure is sufficient for compensation of instrument misalignments.

Acknowledgements

The research presented in this study was made possible by funding from the H2020 MSCA FlexCT IF (GA 752672), the FP7 MSCA INTERAQCT ITN (GA 607817), and the FWO-SBO MetroFleX project (GA S004217N). Furthermore, the authors thank Dr. Suren Chilingaryan at the Karlsruhe Institute of Technology (KIT) for providing computational resources.

References

[1] De Chiffre L, Carmignato S, Kruth JP, Schmitt R, Weckenmann A (2014) Industrial Applications of Computed Tomography. *CIRP Annals - Manufacturing Technology* 63(2):655–677.
[2] Kruth JP, Bartscher M, Carmignato S, Schmitt R, Chiffre L, De Weckenmann A (2011) Computed tomography for dimensional metrology. *CIRP Annals - Manufacturing Technology* 60(2):821–842.
[3] Ferrucci M, Ametova E, Carmignato S, Dewulf W (2015) Evaluating the Effects of Detector Angular Misalignments on Simulated Computed Tomography Data. *Precision Engineering* 45:1–12.
[4] Ferrucci M, Leach RK, Giusca CL, Carmignato S, Dewulf W (2015) Towards Geometrical Calibration of X-ray Computed Tomography Systems — A Review. *Measurement Science and Technology* 26:1–30.
[5] Hermanek P, Ferrucci M, Dewulf W, Carmignato S (2017) Optimized Reference Object for Assessment of Computed Tomography Instrument Geometry. *7th Conference on Industrial Computed Tomography* 7–8.
[6] Deng L, Xi X, Li L, Han Y, Yan B (2015) A Method to Determine the Detector Locations of the Cone-beam Projection of the Balls' Centers. *Physics in Medicine and Biology* 60:9295–9311.
[7] Mathworks (2010) *Global Search Class*. Retrieved from: https://www.mathworks.com/help/gads/globalsearch-class.html.
[8] Feldkamp LA, Davis LC, Kress JW (1984) Practical Cone-beam Algorithm. *Journal of the Optical Society of America* 1(6):612–619.
[9] Stolfi A, De Chiffre L (2016) 3D Artefact for Concurrent Scale Calibration in Computed Tomography. *CIRP Annals - Manufacturing Technology* 65(1):499–502.